Analyst

PAPER

View Article Online
View Journal | View Issue

Cite this: *Analyst*, 2014, **139**, 4820

Simultaneous multiplexed quantification of nicotine and its metabolites using surface enhanced Raman scattering†

Omar Alharbi, Yun Xu and Royston Goodacre*

Received 15th May 2014
Accepted 24th July 2014

DOI: 10.1039/c4an00879k

www.rsc.org/analyst

The detection and quantification of xenobiotics and their metabolites in man is important for drug dosing, therapy and for substance abuse monitoring where longer-lived metabolic products from illicit materials can be assayed after the drug of abuse has been cleared from the system. Raman spectroscopy offers unique specificity for molecular characterization and this usually weak signal can be significantly enhanced using surface enhanced Raman scattering (SERS). We report here the novel development of SERS with chemometrics for the simultaneous analysis of the drug nicotine and its major xenometabolites cotinine and *trans*-3′-hydroxycotinine. Initial experiments optimized the SERS conditions and we found that when these three determinands were analysed individually that the maximum SERS signals were found at three different pH. These were pH 3 for nicotine and pH 10 and 11 for cotinine and *trans*-3′-hydroxycotinine, respectively. Tertiary mixtures containing nicotine, cotinine and *trans*-3′-hydroxycotinine were generated in the concentration range 10^{-7}–10^{-5} M and SERS spectra were collected at all three pH values. Chemometric analysis using kernel-partial least squares (K-PLS) and artificial neural networks (ANNs) were conducted and these models were validated using bootstrap resampling. All three analytes were accurately quantified with typical root mean squared error of prediction on the test set data being 5–9%; nicotine was most accurately predicted followed by cotinine and then *trans*-3′-hydroxycotinine. We believe that SERS is a powerful approach for the simultaneous analysis of multiple determinands without recourse to lengthy chromatography, as demonstrated here for the xenobiotic nicotine and its two major xenometabolites.

Introduction

Raman spectroscopy is a powerful physicochemical technique that can be used to generate molecular specific information about a sample thereby allowing unambiguous analyte characterization.[1] This is particularly important for the detection, identification and quantification of legal drugs and illicit substances. Many studies using Raman spectroscopy have concentrated on the identification of drugs of abuse.[2–5]

Whilst Raman spectroscopy is a very useful technique and can be deployed in a portable manner, the signal from the normal Raman process is inherently weak. This signal can be significantly increased using either resonance Raman or surface enhanced Raman scattering (SERS). In SERS the analyte has to be in contact or microscopically close to a roughened metal surface;[6–10] and for quantitative analysis colloidal preparations of silver or gold nanoparticles are usually employed.[11,12] Our initial work on SERS was aimed at bacterial characterisation[13,14] and more recently we have been optimising SERS for trace detection of microbial metabolites,[12] carcinogens,[15] human drugs[16] as well as illicit materials and legal highs.[17,18]

To date most drug detection studies have concentrated on single analytes, and for illicit substance detection have been limited to the detection of the specific xenobiotic rather than any xenometabolites that may be found when the drug is consumed and detoxified in the liver. The latter is important in order to establish long-term abuse where the drug may no longer be present within a human body fluid (blood or urine) but drug metabolites may still be found. In order to measure drugs and their metabolites chromatography linked with mass spectrometry is typically used.[19] Although this allows for accurate quantification and analyte identification (when matched with a known standard) GC-MS and LC-MS are both labour intensive and cannot yet be deployed remotely. We believe that SERS offers considerable potential for drug detection and quantification and this approach can readily be coupled with portable Raman spectrometers.[12]

If one considers the xenobiotic nicotine, immediately after smoking ~10% of the inhaled nicotine is found in the blood.[20] Nicotine has typical pharmacodynamics where it is very quickly

School of Chemistry, Manchester Institute of Biotechnology, University of Manchester, 131 Princess Street, Manchester, M1 7DN, UK. E-mail: roy.goodacre@manchester.ac.uk

† Electronic supplementary information (ESI) available. See DOI: 10.1039/c4an00879k

convert to cotinine (75% conversion) and cotinine is subsequently converted to *trans*-3′-hydroxycotinine, and a few hours after smoking these appear in blood and urine.[20] Indeed the immediate xenometabolite cotinine is highest in the liver and found at reasonable levels in urine.[20]

The kinetics of nicotine is interesting and this was therefore chosen as a suitable model system for SERS analysis of a drug and its metabolites. This would allow us to establish if SERS can be used to detect and quantify multiple analytes simultaneously without recourse to complicated and time consuming chromatographic separation. Although SERRS has been used for the multiplexed detection of labelled analytes,[21,22] as well as quantification,[23] no study has used non-labelled materials (*i.e.*, SERS) for multiplexed quantitative detection of multiple determinands. Here we show that SERS can be combined successfully with chemometrics and this allows for the quantitative analysis of the drug nicotine and its major metabolites cotinine and *trans*-3′-hydroxycotinine.

Experimental

Chemicals

The reagents used in this investigation were: silver nitrate >99%, tri-sodium citrate, potassium nitrate, nicotine ≥99%, cotinine ~98% and *trans*-3′-hydroxycotinine, all of which were purchased from Sigma-Aldrich (Dorset, UK) and supplied as racemates. Acetic acid (analytical reagent grade) was purchased from Fisher Scientific Company (Loughborough, UK) sodium hydroxide standard solution 0.1 mol L^{-1} purchased from Riedel de-Haen Company (Seelze, Germany).

SERS colloid preparation

Colloids were prepared using the Lee and Meisel method.[24] Briefly, 90 mg of silver nitrate was dissolved in 500 mL of deionised water, after which the solution was heated to boiling point. 10 mL of 1% aqueous solution of tri-sodium citrate was added to the boiling silver nitrate solution drop by drop while the solution was vigorously stirred. The mixed solution was kept boiling for a further 10 min. A green-grey silver colloid was obtained, which proved to be stable for several weeks. The colloid was assessed using UV-visible spectroscopy and electron microscopy (data not shown) and was very similar to that synthesised by us previously.[18,25]

Raman spectroscopy

Raman spectra were obtained using a DeltaNu® Advantage 200A (DeltaNu Inc, Laramie, Wyoming, WY, USA) portable Raman probe, equipped with a HeNe laser operating at 633 nm giving a power of approximately 3 mW at the sample. The spectral range is 200 to 3400 cm^{-1} with a spectral resolution of 8 cm^{-1}. Daily calibration of the instrument was achieved by obtaining the Raman spectrum of polystyrene using the calibration routine built into the instrument manufacture's software. The spectrometer was controlled using DeltaNu, Nu Spec™ software.

pH profiling

In order to optimise the SERS signal we modified the pH of the sample/colloid mixture. In this process each of the three analytes (nicotine, cotinine and *trans*-3′-hydroxycotinine) were analysed separately and 200 μL of these 2×10^{-3} M solutions were mixed with 200 μL colloid. After this the pH was adjusted by the addition of aqueous solutions of 1 M of acetic acid and 0.1 M sodium hydroxide and the range used was from 1–12 in approximately 1 pH steps (±0.1). Next 50 μL 1 M NaCl was added to initiate aggregation, this was vigorously vortexed for 10 s and SERS measurements were immediately collected for 30 s.

For each of the three analytes each pH condition was assessed three times. Five readings were recorded for each preparation. Therefore each condition comprised 15 replicates. The areas under the pyridine vibration at 1030 cm^{-1} were calculated, averaged and plotted against each of the pH conditions investigated. The use of this peak at 1030 cm^{-1} was only to ascertain the overall SERS response for each of the analytes, as this is a vibration that is common to nicotine, cotinine and *trans*-3′-hydroxycotinine and can not be used to differentiate between the three molecules.

Analysis of tertiary mixtures

For the simultaneous quantification of the three analytes, tertiary mixtures were prepared. In preliminary studies the linear response range of SERS *versus* analyte concentration was estimated, and this was found to be 1×10^{-7} M – 1×10^{-5} M. All tertiary mixtures contained the same number of molecules and this was set to 1×10^{-5} M.

The range for each of the three analytes with these mixtures was from 0–100% (in 10% steps; equivalent of one serial dilution); while the total volume of each of the mixtures was kept at 200 μL. In total 66 mixtures were prepared and Table S1† provides an illustration of the molarity of the [nicotine–cotinine–*trans*-3′-hydroxycotinine] mixtures along with their preparation from working stock solutions.

Data analysis

In order to quantify the level of each of the three analytes supervised learning was used. In this process the algorithm is provided with the SERS spectra from mixtures along with the know levels of each of the three analytes. The goal of the algorithm is to estimate the analyte concentrations from the SERS spectra and this is carefully validated (*vide infra*).

The most popular quantitative multivariate algorithm is partial least squares (PLS) regression and this was initially used. However, the predictions for nicotine, cotinine, *trans*-3′-hydroxycotinine was very poor (data not shown) and alternative methods were needed. This suggests that the nature of SERS means that the direct correlation between the SERS spectra and the relative concentrations of the three analytes are not likely to be linear. Therefore we employed two commonly used non-linear regression models to model such correlations, these included artificial neural networks (ANNs) and kernel partial least squares (K-PLS).

Considering different analytes may have different optimal pHs (as indeed was found to be the case) we built regression models using the spectra from each unique pH and also combined the SERS spectra from all the three pH conditions. For each pH we also build two types of models, one was used to predict a single analyte and the other to predict all three analytes simultaneously.

The ANN models consisted of 3 layers: the input layer, the hidden layer and the output layer. The input layer contains the same number of nodes as the number of variables (*i.e.* wavenumber shifts) and this was 200–3400 cm^{-1}, the hidden layer contained 20 nodes and the output layer comprised either a single node (the model which predicted one analyte only) or 3 nodes (the model which predicted three analytes simultaneously). Thus the architecture of these ANNs were either 1024-20-1 or 1024-20-3 for each of the pH conditions. When all three SERS spectra (3 × 1024) were used as the input layer the network topology was 3072-20-1 or 3072-20-3.

The K-PLS models were built using a radial basis function kernel and, similar to the ANN models, PLS-1 models were built to predict a single analyte and PLS-2 models were built to predict the three analytes simultaneously.

In order to test the validation of the regression models a bootstrapping random resampling procedure was employed. In each bootstrapping iteration, n samples (n = total number of samples) were randomly selected with replacement (*i.e.*, one particular sample could be selected multiple times) and used as the training set. The samples which had not been selected at all were used as the test set. Within the training sets 70% of samples were used for training (*i.e.*, the inner training set), and the remaining 30% samples from the training data were used as the validation/tuning set. The regression model was built on the inner training set and the model parameters (*e.g.*, the kernel parameters and the number of latent factors in the K-PLS) were tuned by using the validation set. The model parameters which yielded the best prediction accuracy of the validation set were chosen for the final regression model and this model was then applied to the test sets from the bootstrap selections. A total number of 1000 bootstrapping iterations were performed and the prediction accuracies of these test set iterations were then averaged and reported. The prediction accuracies were presented in terms of validated correlation coefficient Q^2 and root mean square error of prediction (RMSEP) as in eqn (1) and (2).

$$Q^2 = 1 - \frac{\sum_{i=1}^{n} \left(\hat{y}_i - y_i\right)^2}{\sum_{i=1}^{n} \left(y_i - \bar{y}\right)^2} \quad (1)$$

$$\mathrm{RMSEP} = \sqrt{\frac{\sum_{i=1}^{n} \left(\hat{y}_i - y_i\right)^2}{n}} \quad (2)$$

where $\hat{y}_i$ is the predicted relative concentration of sample i, y_i is the actual relative concentration of sample i, $\bar{y}$ is the averaged relative concentration of all the samples in the test set and n is the total number of samples in the test.

Results and discussion

Preliminary studies

Preliminary tests were carried out to optimize SERS on the three analytes. As nicotine, cotinine and *trans*-3′hydroxycotinine all contain a pyridine ring we expect the colloid to interact through the nitrogen in the ring, as this could become positively charged by protonation and therefore come close to the silver nanoparticles (NPs), as these NPs possess an overall negative charge due to the citrate ions on their surface. Previous workers had used NaCl as an aggregating agent for detection of nicotine[26] and we therefore started with this to aggregate our analyte–sol mixtures.

For SERS to be effective it is vital that a suitably rough silver surface is generated and this takes time to form during aggregation. We therefore optimized the time at which to start recording the spectra after the addition of 1 M NaCl. The maximum SERS response from the pyridine ring vibration at 1030 cm^{-1} was after 45 min (data not shown). However, this is clearly too long and time consuming for running experiments where many samples will be analysed. Thus a different approach was attempted, and this included changing the pH of the analyte-sol mixtures before the addition of the aggregating agent.

SERS and pH profiling

Fig. 1 depicts the variation in the Raman signal intensity *versus* Raman shift from the 633 nm laser for nicotine at the different pH conditions investigated. Similar profiles using the same conditions for the cotinine and *trans*-3′-hydroxycotinine were also conducted (spectra not shown). It is clear from Fig. 1 that the SERS spectra of nicotine changes as a function of the pH of the sample.

It is very striking that a peak at 890 cm^{-1} was observed for nicotine but only at pH 1. Visual inspection of all samples (including cotinine and *trans*-3′-hydroxycotinine) at pH 1 showed that instead of a green/grey-milky suspension the samples had rapidly turned black (data not shown). This suggests that the silver has been oxidised and the sol was also seen to precipitate. This was not observed from pH 2–12.

Nicotine is a diprotic base with two pK_a values: the first pK_a is 3.12 for the pyridine ring and the second pK_a is 8.02 for the pyrrolidine ring.[27] The two nitrogen atoms in nicotine have a lone pair of electrons that can be donated to a proton. The lone pair of electrons in the pyrrolidine ring is more readily available for protonation than the lone pair on the nitrogen of the pyridine ring, since these take part in the resonance of the pyridine ring. It has been suggested that the protonation of nicotine is within a pH dependent equilibrium system.[28] As the pH changes from acidic to alkaline conditions the protonation of nicotine will be different and this is shown in Fig. 2 where in highly acidic conditions (<pH 3) both nitrogens are protonated, between *ca.* pH 3–8 nicotine is mono-protonated, and >pH 8 nicotine is non-protonated.

Even though the analyte-colloid mixtures at pH 1 are not really appropriate for SERS it is possible that the presence of the

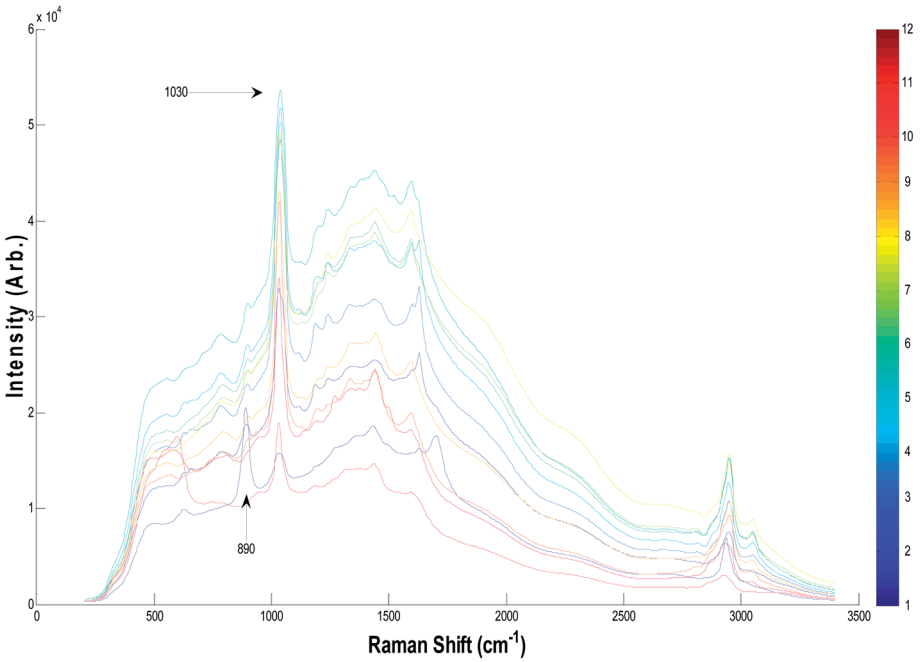

Fig. 1 SERS spectra from pH profiling experiments for nicotine (2×10^{-3} M). The pH was adjusted prior to SERS acquisition from 1–12 in ~1 (±0.1) pH unit steps using acetic acid and NaOH. Spectra were collected for 30 s using 633 nm excitation, with ~3 mW on the sample. Average spectra are displayed from 15 independent collections. Arrows indicate the 890 cm^{-1} vibration and the pyridine ring vibration at 1030 cm^{-1}. The colour scale bar represents the pH of the conditions used for SERS and these colours the lines used to represent the different spectra.

two-protonated nicotine species could be the reason behind the appearance of the peak 890 cm^{-1} in SERS, which is also present to a much lesser extent from pH 2–9, but disappears >pH 9. It is also possible that at low pH when both the pyridine and pyrrolidine are protonated that nicotine may be forced to lie flat on the surface, and whilst there is no direct evidence of this, this again could explain this 890 cm^{-1} peak.

The variation of the peak area (1030 cm^{-1}) associated with the pyridine ring as a function of the pH of the mixtures studied for each of the nicotine, cotinine and *trans*-3-hydroxycotinine are shown in Fig. 3. Nicotine spectra show that the maximum peak area is obtained at around pH 3. However, further investigation is required in pH range 2–4 in order to verify the exact optimum of the peak area with pH (but one would assume it will be close to the pH 3.1 as this is the pK_a of the pyridine ring). This spectrum further reveals no appreciable change in the intensity of the peak area between pH 4–8. One is tempted to work within this regime of pH, although at a sacrificed of around 13% in the intensity when compared with that at pH 3, due to the experimental difficulty encountered in adjusting the pH of solution.

For nicotine between pH 4–8 protonation occurs in the pyrrolidine ring (Fig. 2) suggesting this could result in nicotine binding to the surface through this nitrogen rather than the one on the pyridine ring. A small peak at this pH range is seen at 900 cm^{-1} (Fig. 1) which could be due to pyrrolidine. In addition, as vibrations perpendicular to the surface are more enhanced this should result in a change in the relative intensity of the peaks due to the change of conformation on the surface.

As for the cotinine results, no significant change is observed in the peak area in the range of pH 1–7; however, an intense increase in pyridine peak intensity is observed as one moves from pH 8 to pH 9–10, after which a decline in the intensity is noticed as the pH increases to 12. In contrast to that of nicotine and cotinine, two distinct peak area maximum are observed at pH 3 and pH 11 in SERS of *trans*-3′-hydroxycotinine. In both cases a decline is seen with an increase of the pH after reaching the peak maximum.

The pK_a for both cotinine and *trans*-3′-hydroxycotinine is 4.5, and this is again due to the nitrogen within the pyridine ring being protonated. This could explain the slight rise in the

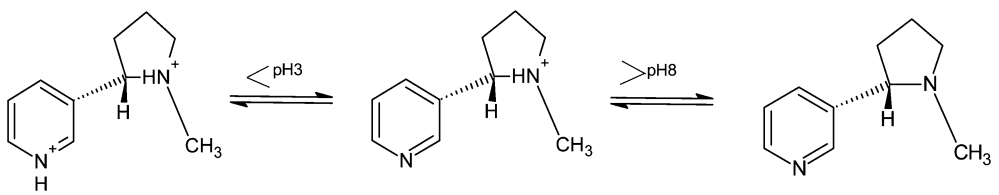

Fig. 2 Scheme showing the ionisation of nicotine in acidic and basic conditions.

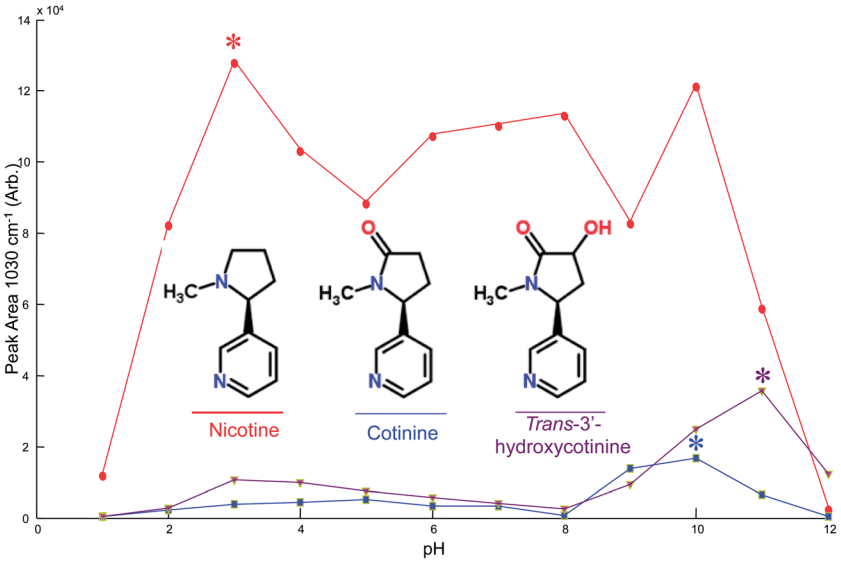

Fig. 3 pH profiling results from the 3 analytes under investigation. The peak area averages at 1030 cm^{-1} were calculated from the 15 replicate spectra at each pH for each of the analytes. The asterisks show the point where the optima signals for nicotine, cotinine and *trans*-3′-hydroxycotinine occurs and these were used for future investigations. Structures for the analytes are shown and these are generated from ChemSpider (http://www.chemspider.com).

pyridine ring vibration from pH 3–5, as again the availability of a lone pair of electrons on the nitrogen atom of pyridine ring will be involved in the increased adsorption of these species on to the silver colloid surface.

Under alkaline conditions for both cotinine (pH 10) and *trans*-3′-hydroxycotinine (pH 11) there is a significant increase in the 1030 cm^{-1} pyridine peak (Fig. 3 indicated by *); the same could also be observed for nicotine at pH 10. This is an interesting observation for which we have no current explanation; this could be due to citrate being removed from the surface of the NPs and thereby vacating the surface for absorption by the pyridine-containing analytes. However, there is no direct evidence for this and liquid chromatography-mass spectrometry of the solution would not be possible given the excess of citric acid used in the reduction of the Ag^{2+} to Ag (0). We do stress that as each spectrum was collected 15 times (5 repeats from 3 different preparations) this observation is real and establishes the optimum pH conditions for each of the three analytes.

From the results obtained above one can conclude that the pH of the mixture has an important impact on the intensity of the SERS response. All the analytes investigated in this study contain nitrogen which could be found in protonated or unprotonated forms under the different pH values that have been used in the study. At acid pH the protonated forms will dominate, and as the pH increase the number of protonated species will be reduced. It is known that the extent of interaction (bonding) of such molecules with the silver colloid surface is affected by the presence or absence of these protonated forms, as this will affect the availability of lone pairs of electrons onto the nitrogen atoms for adsorption of the species onto silver colloid surface which in turn impact on the intensity of Raman.

Establishment of the linear working range for SERS

Based on the above results three calibration curves for nicotine, cotinine and *trans*-3′-hydroxycotinine were carried out using each analyte diluted from 1×10^{-10} M – 1×10^{-4} M where the pH was adjust to 3, 10 and 11 for nicotine, cotinine and *trans*-3′-hydroxycotinine, respectively. This allowed the establishment of the concentration range at which the signal response for the 1030 cm^{-1} peak area from the pyridine ring was linear with respect to the analyte concentration.

Five reading were recorded for each concentration and the average peak intensity was plotted *versus* the analyte concentrations (data not shown). The results revealed that the signal was linear for nicotine between 1×10^{-7} M to 1×10^{-5} M, and for both cotinine and *trans*-3′-hydroxycotinine was slightly lower from 1×10^{-8} M to 1×10^{-5} M.

Quantitative analysis in tertiary mixtures

As detailed in the Materials and Methods section tertiary mixtures of nicotine, cotinine and *trans*-3′-hydroxycotinine were prepared three times at the three different pH (*viz.* pH 3, 10 and 11), and each sample was analysed five times. Having established that the linear SERS response range these mixtures was 1×10^{-7} M – 1×10^{-5} M 66 mixtures were prepared in '10%' steps (see for example as in Table S1†). The total number of molecules was always 1×10^{-5} M, and this was performed so that the number of molecules competing for the silver surface was always constant.

In the above optimization studies (in terms of pH and linear working range) the peak area at 1030 cm^{-1}, which is associated with the pyridine ring, was only used to illustrate the overall SERS enhancement effect for nicotine, cotinine and *trans*-3′-hydroxycotinine and we stress that this single vibrational mode

cannot be used to differentiate between these three different analytes. Illustrations of the SERS spectra for each of the individual analytes at the three different pH conditions are provided in Fig. S1–S3† along with a mixture of all three molecules together (Fig. S4†). It is clear from these plots that differentiation by eye is very difficult and that the mixture spectra change dramatically as a function of pH, and for the illustrated mixture containing 60 : 20 : 20 (nicotine : cotinine : *trans*-3′-hydroxycotinine) that pH 3 is quite featureless; other mixtures show different effects (data not shown), again highlighting the complexity of these analyses.

Initial analyses established that PLS regression was not able to produce very good predictions of these three pyridine ring-containing molecules. This suggests that the mapping from input SERS spectra to output analyte concentration(s) was not linear, therefore we assessed non-linear mapping/regression algorithms. ANN and K-PLS were used and all models were validated using multiple testing *via* bootstrapping. As there were 3 analytes to be quantified at 3 different pH optima a series of 16 chemometric models were generated. These used: (i) the single SERS input with a single analyte output prediction for each pH (total = 9 models); (ii) the single SERS input with 3 analyte outputs for each pH (3 models); alternatively, all three SERS spectra were combined and used as the input with and the output was either (iii) a single analyte (3 models; Fig. S5†) or (iv) all 3 analytes (a single model; illustrated in Fig. 4).

As an example, the results of an ANN are depicted in Fig. 4 for all three SERS spectra combined with a single model using 3 output nodes. It is clear from this figure that nicotine, cotinine and *trans*-3′-hydroxycotinine are all predicted very well and follow the expected $y = x$ line. Closer inspection suggests that nicotine is predicted with better accuracy than cotinine and *trans*-3′-hydroxycotinine and this may be expected as the relative signal strength for nicotine was higher than the other two analytes (Fig. 3).

The results for both the ANNs and K-PLS are shown in Table 1 for the single output predictions and in Table S2† for when all three analytes are simultaneously predicted. As detailed in the Materials and Methods section all the predictions are on the test sets from the bootstrap results and these tables show the average predictions for the 1000 resamplings performed. These tables provide the Q^2 which is a measure of the correlation coefficient between the expected and predicted analyte concentrations, as well as the RMSEP (root mean square error of

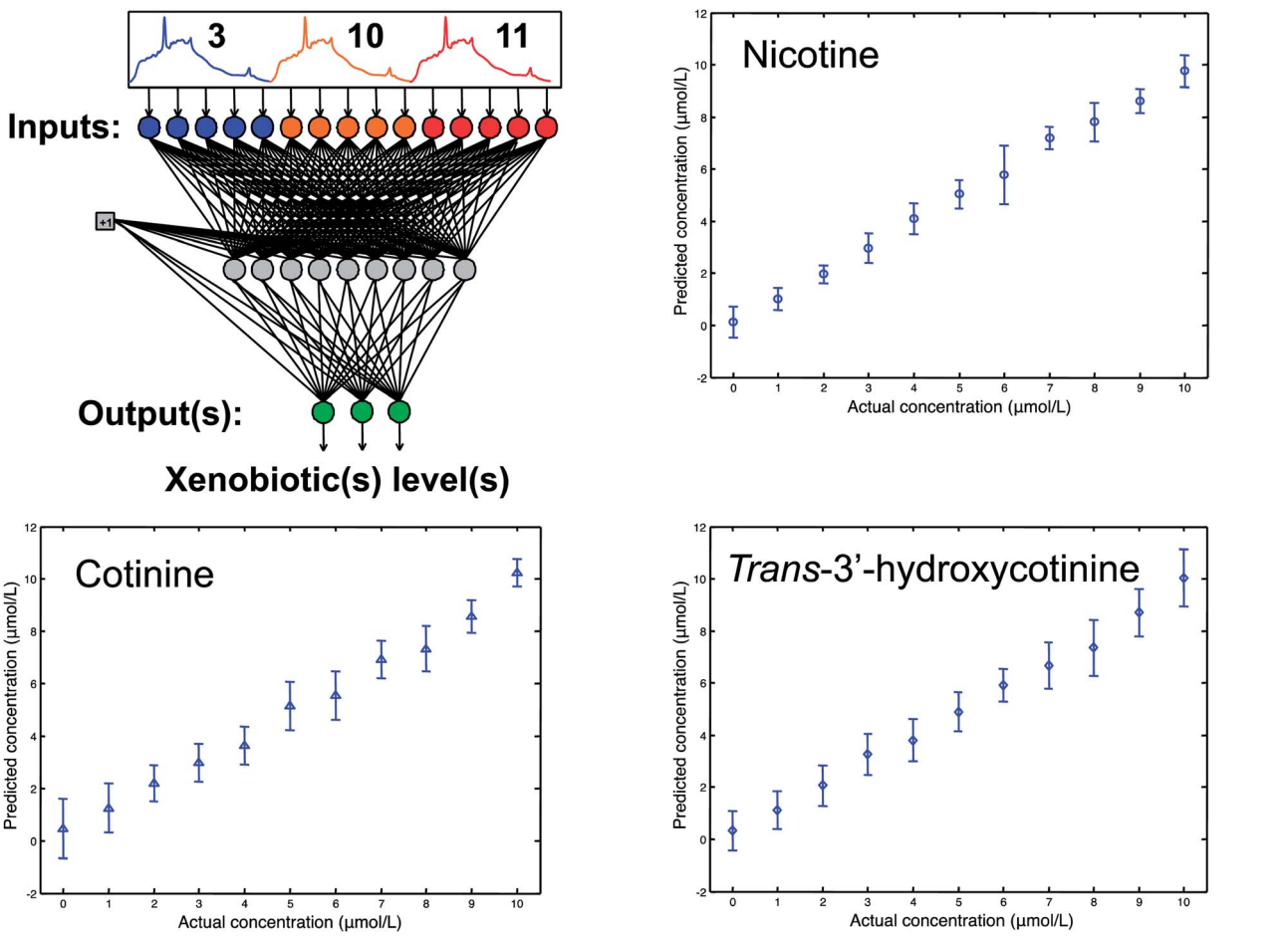

Fig. 4 Cartoon of the artificial neural network (ANN) architecture used which comprised 3072 (3 × 1024) inputs 20 nodes in the hidden layer and 3 output nodes, with the ANN predictions trained with the input SERS data from mixtures of nicotine, cotinine and *trans*-3′-hydroxycotinine at all three pH conditions. Points show the averages of the test data only with standard deviation error bars.

Table 1 Chemometric model predictions for nicotine, cotinine and *trans*-3′-hydroxycotinine. In these predictions a single output node was used in each of the ANNs

		Nicotine		Cotinine		*Trans*-3′-hydroxy cotinine	
		Q^2	RMSEP	Q^2	RMSEP	Q^2	RMSEP
pH = 3	ANN	0.9176	7.7153	0.5054	18.9055	0.6123	16.7196
	K-PLS	0.9001	8.5703	0.4995	19.0315	0.6066	16.8861
pH = 10	ANN	0.9591	5.4378	0.8775	9.5897	0.8105	11.6987
	K-PLS	0.9512	5.9171	0.8687	9.8734	0.8054	11.9003
pH = 11	ANN	0.9382	6.6793	0.7911	12.2670	0.8122	11.6462
	K-PLS	0.9297	7.1061	0.7845	12.4158	0.8015	11.9728
Combined	ANN	0.9519	5.8915	0.8869	9.0397	0.9092	8.0987
	K-PLS	0.9489	6.0487	0.8858	9.1903	0.9017	8.4909

prediction) for the test sets. Thus better models will have a Q^2 close to 1 and have a low RMSEP.

It can be seen that under the optimal pH condition for each analyte there was generally very good agreement between the actual concentration and the predicted concentration of each of the three analytes. For all predictions the ANNs outperformed K-PLS. This may be due to ANNs ability to perform superior non-linear mapping from an input layer (*i.e.* SERS spectra) to an output layer (*i.e.* drug or drug metabolite level) when a single hidden layer is used.[29,30] In addition, for both ANNs and K-PLS the models which were calibrated to predict a single analyte (Table 1) generated better results than the corresponding models which predicted all three analytes simultaneously (Table S2†).

It can be seen that the lowest error in nicotine quantification was 5.4% RMSEP ($Q^2 = 0.96$) and this is when SERS was conducted at pH 10 and calibrated with an ANN when a single output node was employed. For cotinine and *trans*-3′-hydroxycotinine the lowest errors were also with an ANN containing a single output and were 9.0% and 8.1% respectively ($Q^2 = 0.89$ and 0.91); in both instances the SERS spectra from all three pH conditions were combined and used for modelling. The nicotine RMSEP for the same combined SERS input (*i.e.*, the 3072-20-1 ANN) was 6.6% ($Q^2 = 0.95$) and perhaps this model was a good compromise for the prediction of all three analytes. Moreover, it is clear from Table S2† that a good compromise for good overall predictions using ANNs for modelling for nicotine, cotinine and *trans*-3′-hydroxycotinine are when SERS spectra were collected at pH 10; a finding that is also seen for K-PLS (Table S2†).

In conclusion, we have developed colloid-based SERS for the analysis of three analytes in tertiary mixtures without recourse to prior chromatographic separation. Raman spectra were obtained using a portable Raman probe (DeltaNu instrumentation) and this illustrates that this approach could be deployed remotely. When the data generated were analysed with ANNs this allowed for the simultaneous quantification of the drug nicotine and its major drug metabolites cotinine and *trans*-3′-hydroxycotinine. Future studies will be conducted to extend this to testing from complex biological matrices, including blood and urine, where we expect that we shall have to use selective solvent extraction to recover these pyridine-based chemical species.

Acknowledgements

OA thanks forensic and toxicology centre and ministry of health in Saudi Arabia for funding. YX thanks Cancer Research UK for funding and RG is indebted to UK BBSRC for financial support.

References

1 D. I. Ellis, D. P. Cowcher, L. Ashton, S. O'Hagan and R. Goodacre, *Analyst*, 2013, **138**, 3871–3884.
2 M. J. West and M. J. Went, *Drug Test. Anal.*, 2010, **3**, 532–538.
3 S. E. J. Bell, D. T. Burns, A. C. Dennis, L. J. Matchett and J. S. Speers, *Analyst*, 2000, **125**, 1811–1815.
4 A. G. Ryder, G. M. O'Connor and T. J. Glynn, *J. Raman Spectrosc.*, 2000, **31**, 221–227.
5 N. Milhazes, F. Borges, R. Calheiros and M. P. M. Marques, *Analyst*, 2004, **129**, 1106–1117.
6 M. Fleischmann, P. J. Hendra and A. J. McQuillan, *Chem. Phys. Lett.*, 1974, **26**, 163–166.
7 D. L. Jeanmaire and R. P. Van Duyne, *J. Electroanal. Chem. Interfacial Electrochem.*, 1977, **84**, 1–20.
8 M. Moskovits, *Rev. Mod. Phys.*, 1985, **57**, 783.
9 S. Nie and S. R. Emory, *Science*, 1997, **275**, 1102–1106.
10 W. E. Smith, *Chem. Soc. Rev.*, 2008, **37**, 955–964.
11 S. E. J. Bell and N. M. S. Sirimuthu, *J. Am. Chem. Soc.*, 2006, **128**, 15580–15581.
12 D. P. Cowcher, Y. Xu and R. Goodacre, *Anal. Chem.*, 2013, **85**, 3297–3302.
13 R. M. Jarvis and R. Goodacre, *Anal. Chem.*, 2004, **76**, 40–47.
14 R. M. Jarvis and R. Goodacre, *Chem. Soc. Rev.*, 2008, **37**, 931–936.
15 W. Cheung, I. T. Shadi, Y. Xu and R. Goodacre, *J. Phys. Chem. A*, 2010, **114**, 7285–7290.
16 C. Levene, E. Correa, E. W. Blanch and R. Goodacre, *Anal. Chem.*, 2012, **84**, 7899–7905.
17 S. Mabbott, A. Eckmann, C. Casiraghi and R. Goodacre, *Analyst*, 2013, **138**, 118–122.
18 S. Mabbott, E. Correa, D. P. Cowcher, J. W. Allwood and R. Goodacre, *Anal. Chem.*, 2013, **85**, 923–931.
19 E. J. Cone, M. Hillsgrove and W. D. Darwin, *Clin. Chem.*, 1994, **40**, 1299–1305.
20 J. Hukkanen, P. Jacob and N. L. Benowitz, *Pharmacol. Rev.*, 2005, **57**, 79–115.
21 K. Faulds, R. Jarvis, W. E. Smith, D. Graham and R. Goodacre, *Analyst*, 2008, **133**, 1505–1512.
22 K. Faulds, F. McKenzie, W. E. Smith and D. Graham, *Angew. Chem., Int. Ed. Engl.*, 2007, **46**, 1829–1831.
23 K. Gracie, E. Correa, S. Mabbott, J. A. Dougan, D. Graham, R. Goodacre and K. Faulds, *Chem. Sci.*, 2014, **5**, 1030–1040.
24 P. C. Lee and D. Meisel, *J. Phys. Chem.*, 1982, **86**, 3391–3395.
25 I. Shadi, W. Cheung and R. Goodacre, *Anal. Bioanal. Chem.*, 2009, **394**, 1833–1838.

26 S. E. J. Bell and N. M. S. Sirimuthu, *Analyst*, 2004, **129**, 1032–1036.
27 L. A. Ciolino, J. A. Turner, H. A. McCauley, A. W. Smallwood and T. Y. Yi, *J. Chromatogr. A*, 1999, **852**, 451–463.
28 J. F. Pankow, *Chem. Res. Toxicol.*, 2001, **14**, 1465–1481.
29 K. Hornik, M. Stinchcombe and H. White, *Neural Network.*, 1989, **2**, 359–366.
30 K. Hornik, M. Stinchcombe and H. White, *Neural Network.*, 1990, **3**, 551–560.